

Generic Contrast Agents

Our portfolio is growing to serve you better. Now you have a *choice*.



FRESENIUS
KABI

[VIEW CATALOG](#)

AJNR

Gd-DTPA enhancement of posterior epidural scar: an experimental model.

J S Ross, S Blaser, T J Masaryk, S E Emory, M Bolesta, J Carter, M Aikawa and M T Modic

AJNR Am J Neuroradiol 1989, 10 (5) 1083-1088

<http://www.ajnr.org/content/10/5/1083>

This information is current as
of May 14, 2025.

Gd-DTPA Enhancement of Posterior Epidural Scar: An Experimental Model

Jeffrey S. Ross¹
 Susan Blaser¹
 Thomas J. Masaryk¹
 Sanford E. Emory²
 Michael Bolesta²
 John Carter^{2,3}
 Masamichi Aikawa³
 Michael T. Modic¹

Because of the tremendous clinical and physiological importance of anterior epidural scar, an easily produced and reproducible model to assess potential pathways for lessening its formation is a necessity. We speculated whether posterior epidural scar (produced by the less complex surgery of laminectomy alone) could be considered equivalent to anterior scar from an imaging standpoint; that is, enhancement following Gd-DTPA irrespective of scar age. Posterior epidural scar in dogs showed the highest degree of enhancement 1 month after surgery, with a rapid decline thereafter out to 4 months postsurgery to a level equivalent to that of paraspinal muscle. Gd-153-DTPA time/activity curves paralleled the Gd-DTPA findings. Light microscopy showed granulation tissue after 1 month, and mature scar with large amounts of collagen 4 months after surgery. Electron microscopy showed tight capillary endothelial junctions.

An appropriate model for epidural scar, which has imaging characteristics similar to human anterior scar, necessitates an extensive lumbar laminectomy with anterior epidural dissection. A simple laminectomy, while easily performed, does not provide a physiologically correct time course of enhancement.

AJNR 10:1083-1088, September/October 1989

A great deal of time and attention has been given to the control of epidural scar formation through placement of fat grafts or with various experimental agents [1-4]. These approaches have commonly used a simple laminectomy model to assess posterior epidural scar [5, 6]. This type of scar, while complicating the initial stage of reoperation, is otherwise not routinely involved in the failed back surgery syndrome, nor given a great deal of consideration in imaging studies [7]. This is in stark contrast to anterior or lateral epidural scar, which is associated with surgically remedial causes of recurrent pain (i.e., recurrent disk herniation) as well as the obviously important anatomy of the exiting nerve roots [8].

Because of the importance of anterior epidural scar, many techniques have been advocated for its diagnosis and distinction from disk material [9-13]. Recent work has demonstrated enhancement of epidural scar by MR following administration of Gd-DTPA in previously operated spines [14]. Anterior epidural scar enhances consistently. Anterior epidural scar has been seen to enhance in patients who had surgery as long as 30 years prior to the Gd-DTPA-enhanced studies. We have previously shown that marked enhancement of epidural scar in dogs (5 months after surgery) in a pattern similar to that seen in humans is secondary to scar vascularity and loose scar capillary endothelial junctions [15]. This model was surgically complex, since it necessitated an extensive laminectomy with dissection anterior to the thecal sac for placement of a plastic constrictive band.

Because of the tremendous clinical and physiologic importance of anterior epidural scar, an easily produced and reproducible model to assess potential pathways for lessening its formation is a necessity. We wondered whether posterior epidural scar produced by the less complex surgery of simple laminectomy could, in fact, be considered equivalent to anterior epidural scar. This equivalence, from

Received October 4, 1988; revision requested December 15, 1988; revision received January 19, 1989; accepted January 29, 1989.

¹ Department of Radiology, University Hospitals of Cleveland, Case Western Reserve University, 2074 Abington Rd., Cleveland, OH 44106. Address reprint requests to J. S. Ross.

² Department of Orthopaedics, University Hospitals of Cleveland, Case Western Reserve University, Cleveland, OH 44106.

³ Department of Pathology, University Hospitals of Cleveland, Case Western Reserve University, Cleveland, OH 44106.

0195-6108/89/1005-1083

© American Society of Neuroradiology

an imaging standpoint should be consistent enhancement irrespective of age, as seen in human anterior scar. To test the hypothesis that posterior scar would enhance consistently despite the time since surgery, we undertook a four-part study in dogs following simply laminectomy: (1) the time course of enhancement of posterior scar with Gd-DTPA was measured over 4 months, (2) the time/activity curves were obtained for posterior epidural scar with Gd-153-DTPA, (3) the histology of posterior scar was assessed with light microscopy, and (4) the ultrastructure of scar, including the endothelial morphology, was assessed with electron microscopy.

Materials and Methods

Animal Model

Ten adult female beagle dogs (12–14 kg) had laminectomy at the L6–L7 level. Epidural scar has been shown to form consistently after laminectomy in dogs [5]. Two dogs were sacrificed after 1 month for histology. The other eight dogs had the imaging studies described below.

Imaging Schemes

Imaging experiments were performed on a 1.5-T Siemens superconducting magnet. Eight dogs were imaged at monthly intervals up to 4 months postsurgery. The dogs were anesthetized with sodium pentobarbital IV, intubated, and then placed supine on a 21-cm-diameter resonator coil centered over the lower lumbar spine. Initially, sagittal spin-echo images 400/13/4, (TR/TE/excitations) with a 4-mm slice thickness and 50% gap were obtained for localization of the axial images at the operative site. Following acquisition of a precontrast axial image at the surgical site, Gd-DTPA was injected intravenously as a bolus (0.1 mmol/kg). Images were obtained every minute for the first 10 min, and then every 5 min up to the end of the examination (45 min). This procedure was repeated at monthly intervals.

The dynamic MR studies were obtained by using a gradient-echo technique (FLASH) with the following parameters: 20/10/8, 60° flip angle, 10-mm slice thickness, and 256 phase-encoded cycles. With the addition of recycling time, images could be obtained every 60 sec. The phase- and frequency-encoded directions were reversed, so flow-related artifact would not project over the spine.

Data Analysis

Signal intensities (SI) were measured from regions of interest (ROI) centered over the posterior epidural scar as well as paraspinal musculature on each pre- and postcontrast image. ROIs included approximately 0.1 cm², and were held constant in position and size as each intensity measurement was taken. Hard-copy images were obtained of the positioning of the axial images and ROIs on each dog at month 1, which were subsequently used to position the imaging sites and ROIs for the remaining 3 months.

Percent contrast enhancement was calculated by using the following formula:

$$\text{enhancement} = \frac{\text{post SI} - \text{pre SI}}{\text{pre SI}} \times 100$$

Standards were not included because of the difficulty in maintaining correct position of the standard on subsequent months, with the inherent field drop-off associated with surface coils.

A sham experiment was performed on dog 256 at 3½ months after surgery to assess signal variability over a 15-min period. A precontrast axial image was obtained, and then saline was injected into a forefoot vein and postinjection images repeated each minute through 10 min postinjection, with a final image obtained at 15 min postinjection. Signal intensities were measured for scar and muscle as above.

Gd-153-DTPA

Two dogs, each at 1 month and 4 months after surgery, were intubated and anesthetized. Surgical dissection was carried down to the epidural scar. Gd-153-DTPA was then injected intravenously and samples were obtained of venous blood, paraspinal musculature, and posterior epidural scar at 1, 3, 5, and 10 min postinjection. At 1 month after surgery the dogs received 20 µCi Gd-153-DTPA, while at 4 months after surgery they received 40 µCi. Sample activity was subsequently counted, and the rate corrected to yield counts/gram tissue for construction of a time/activity curve.

Histology

Two dogs were sacrificed at 1 month and four dogs sacrificed at 4 months after surgery, and samples of posterior epidural scar were obtained. Samples for light microscopy were obtained from each of the six dogs and fixed in 10% formaldehyde embedded conventionally in paraffin. Samples for electron microscopy were obtained from the four dogs sacrificed 4 months postsurgery and were fixed in 2.5% glutaraldehyde buffered to pH 7.4 and 0.1 mol/l sodium cacodylate and 7.5% sucrose for a minimum of 24 hr. Postfixation was performed with 1% osmium tetroxide for 1 hr. Samples were embedded in Epon 812, and portions of interest were cut by using diamond knives and were stained with uranyl acetate. Observations were made on a JEM 100cx electron microscope.

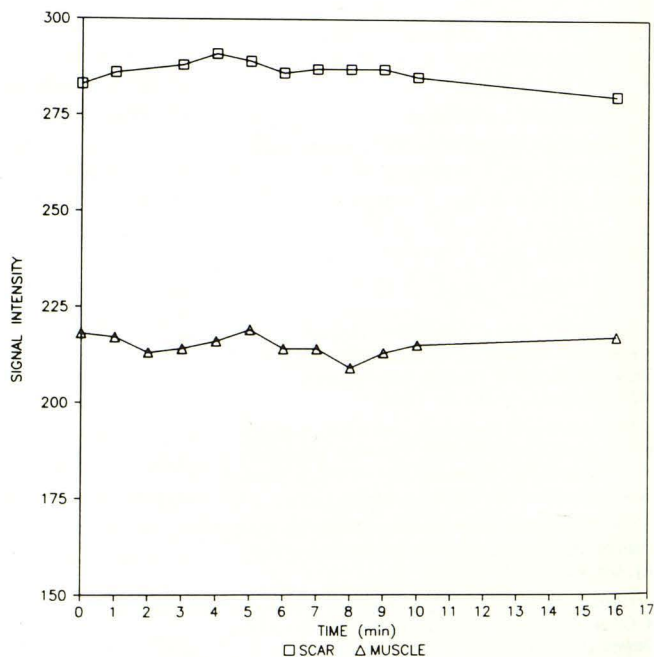
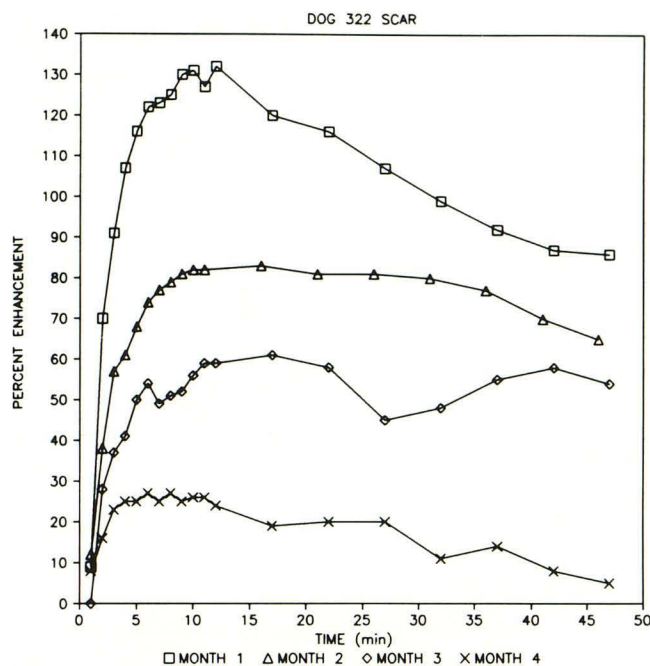
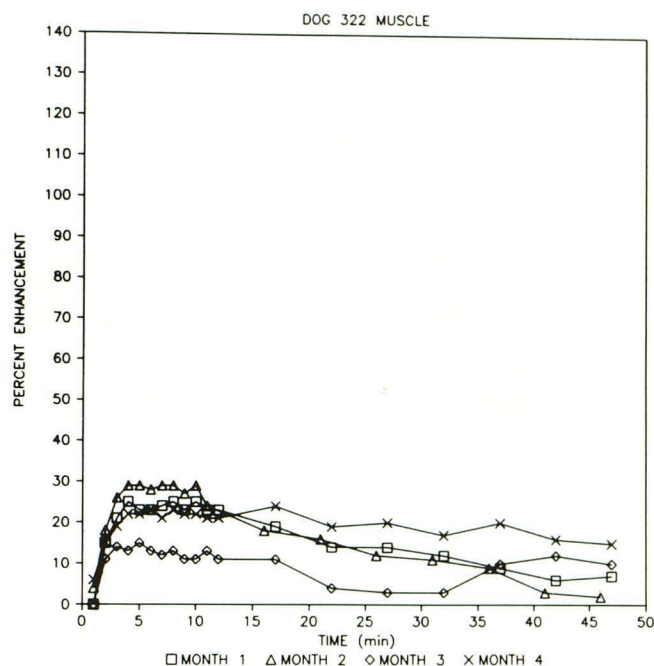


Fig. 1.—Sham experiment shows little signal variation over a 16-min period.



A



B

Fig. 2.—A, Enhancement versus time for posterior epidural scar in dog at 1, 2, 3, and 4 months after surgery. There is greatest enhancement at month 1, with each succeeding month showing less enhancement.

B, Enhancement versus time for paraspinal muscle. There are consistently low levels of enhancement throughout the study period. The month-4 scar curve (A) shows a degree of enhancement similar to paraspinal muscle.

Results

Dynamic MR

Of the 32 MR examinations performed in the eight dogs (four examinations each), 30 were without technical flaws. The month-4 (M4) examination in dog 256 did not have data beyond 20 min postinjection because of motion artifact. Similar problems were encountered in the M2 data in dog 254.

A sham examination was performed in dog 256 at 3½ months after surgery (Fig. 1). This showed minimal variation within the signal intensities over the examination time.

The signal intensities of the posterior epidural scar in the eight dogs showed a consistent trend over the 4-month period. A typical plot is shown in Figure 2A. The M1 enhancement curves showed the highest peaks during the 4-month period (X = 106%, R = 83–132%). Each succeeding month showed overall lower enhancement peaks (M2 X = 77%, R = 70–90%; M3 X = 52%, R = 35–85%; M4 X = 30%, R = 10–80%). There was generally a slow decline in enhancement from the time to peak out to the end of the study at 45 min after injection.

Paraspinal muscle, used as a control, showed consistently low levels of peak enhancement throughout the 4-month period (M1 X = 29%, R = 20–43%; M2 X = 20%, R = 14–25%; M3 X = 21%, R = 14–34%; M4 X = 21%, R = 11–34%). A typical plot is shown in Figure 2B. Times to peak enhancement for scar and muscle are shown in Table 1.

Gd-153-DTPA

The time/activity curves for blood at both 1 and 4 months after surgery showed the typical exponential decrease in

TABLE 1: Time to Peak Enhancement

Month	Scar (S)/ Muscle (M)	Mean (min)	Range (min)
1	S	9	6–12
	M	4	2–8
2	S	10	8–12
	M	6	3–8
3	S	9	6–12
	M	4	2–8
4	S	7	3–15
	M	5	3–7

activity as the gadolinium was cleared from the vascular system (Fig. 3). The time/activity curves for paraspinal muscle and scar paralleled the findings seen with the dynamic MR. That is, at month 1, the overall activity in epidural scar was higher than that of the low-level activity seen with paraspinal muscle. At month 4, paraspinal muscle and scar activity closely paralleled each other throughout the duration of the examination.

Histology

Light microscopy of the epidural scar at month 1 showed areas of granulation tissue with capillaries and plump fibroblasts, as well as additional areas showing more extensive collagen deposition (Fig. 4A). Histology at month 4 showed extensive mature scar composed principally of collagen, with a few intervening capillaries and fibrocytes (Fig. 4B). In two

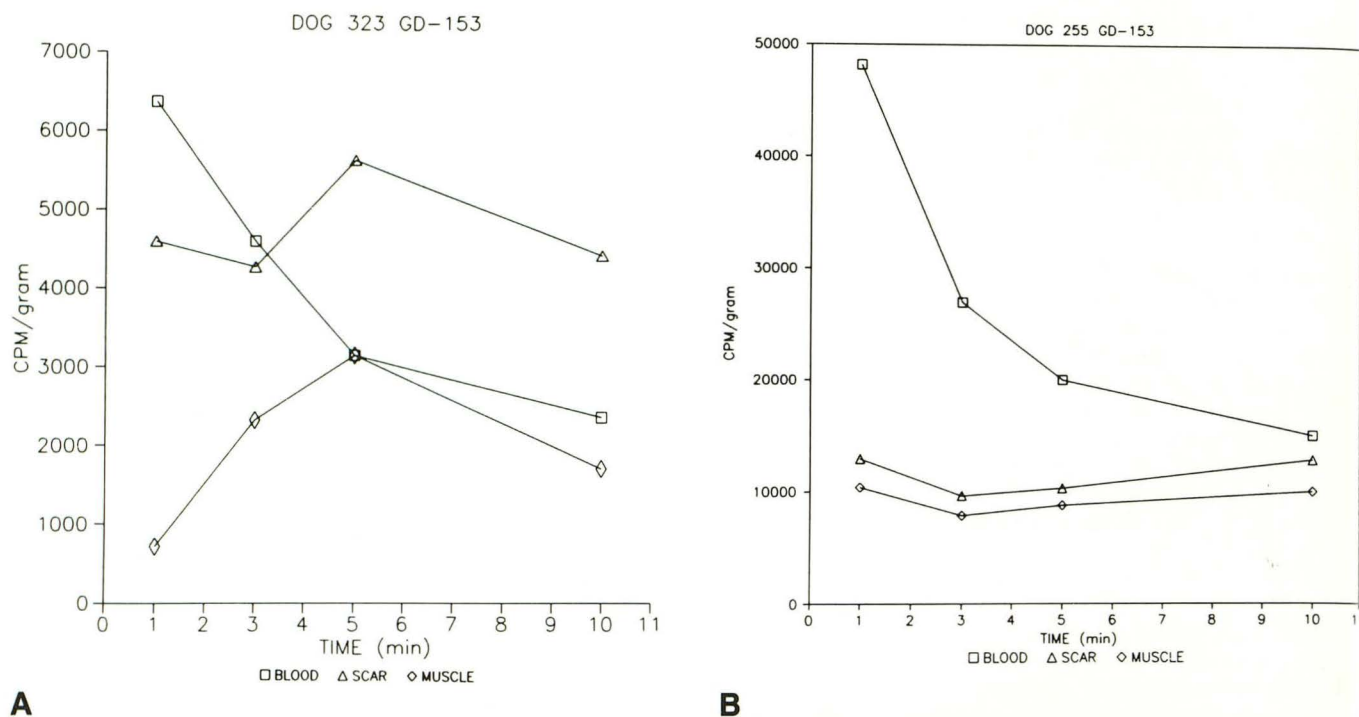


Fig. 3.—A and B, Gd-153-DTPA time/activity curves at 1 month (A) and four months (B) after surgery for blood, posterior epidural scar, and paraspinal muscle. Scar shows a higher level of activity than muscle at 1 month, while scar and muscle have similar low levels of activity at 4 months, paralleling the Gd-DTPA MR experiment (Fig. 2).

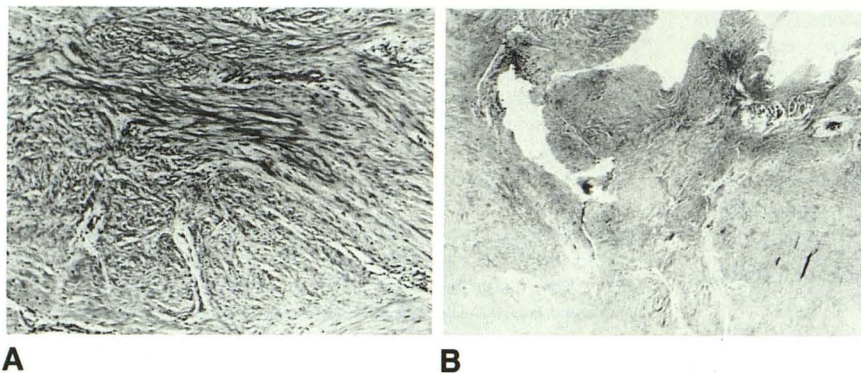


Fig. 4.—A, Light micrograph of posterior epidural scar 1 month after surgery shows several capillaries interspersed between abundant collagen and fibrocytes. (H and E, $\times 100$)

B, Light micrograph of posterior epidural scar 4 months after surgery shows extensive collagen but few small capillaries. (H and E, $\times 50$)

dogs, areas of metaplastic cartilage were seen at the laminectomy site.

Electron microscopy consistently demonstrated tight capillary endothelial junctions seen as electron-dense regions with close apposition of the outer leaflets of the cell membranes (Fig. 5). On only two sections were "loose" type endothelial junctions recognized (Fig. 6) where the outer leaflets of the adjacent cell membranes were less closely approximated to each other. Interspersed between the capillaries were occasional fibrocytes and a large amount of collagen (Fig. 7).

Discussion

This study has demonstrated that a simple laminectomy model in dogs is not appropriate or applicable to the study of

epidural scar in humans since it fails to show persistent enhancement beyond 1 month after surgery. After 1 month, the enhancement of scar decreased rapidly in this dog model and reached a level equivalent to that of paraspinal muscle. The dynamic MR findings were substantiated by the Gd-153-DTPA time/activity curves, which showed scar activity higher than muscle at month 1, but equivalent activity by month 4. In contrast, human anterior and lateral epidural scar shows persistent enhancement after Gd-DTPA administration even years after surgery [14]. In this model, posterior scar behaved more like typical peripheral scar; that is, it underwent rapid cicatrization with increasing amounts of collagen and decreasing amounts of water and vasculature [16]. Electron microscopy showed a "mature" endothelium at 4 months after surgery, with tight endothelial cell junctions. This differs from

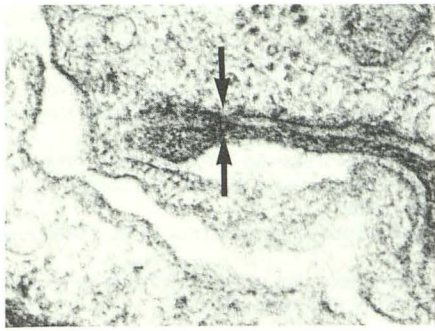


Fig. 5.—Tight dog scar capillary endothelial junction shows close apposition of membrane leaflets (arrows) (electron micrograph $\times 108,000$). The junctions were commonly seen in the month-4 specimens.

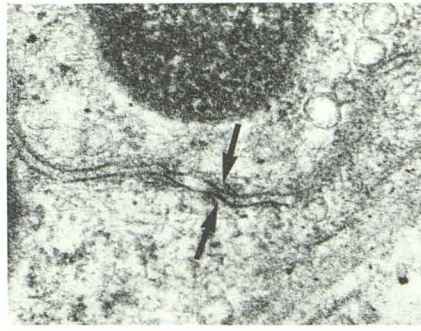


Fig. 6.—“Loose” capillary endothelial junctions, where outer membrane leaflets show increased electron density (arrows) and do not as closely approximate each other. These junctions were rare in the specimens obtained 4 months after surgery (electron micrograph $\times 81,000$).

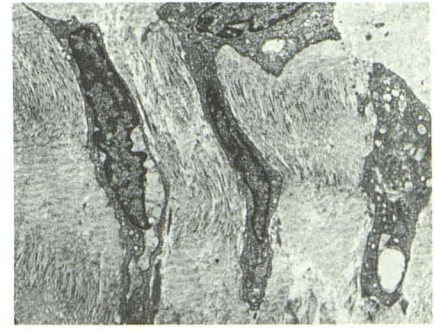


Fig. 7.—Interstice of mature scar shows abundant collagen, demonstrating its typical staining periodicity, and scattered fibrocytes (electron micrograph $\times 6975$).

the leaky junctions that are present in immature scar in both our previous dog model and in humans [15].

Why the disparity in findings between scar in postoperative patients and this dog model? A major consideration is the nature and location of the scar itself. It is apparent that not all scar reacts in the same way over time, and it may be necessary to subdivide epidural scar in part on the basis of location. We postulate that anterior epidural scar cannot be considered to be in an environment that is equivalent to posterior scar. Anterior epidural scar is intimately connected to the function, biomechanics, and disease of the intervertebral disk and adjacent endplates. It is possible that continuing degeneration and/or herniation of the intervertebral disk would cause growth of new anterior scar. In fact, we have seen a mixture of new scar (less than 1 month old histologically) and mature scar in patients with failed back surgery syndrome who had surgery more than 6 months prior to imaging [14]. This suggests a continuing cycle of inflammation and trauma with various ages of scar within the anterior epidural space at any one time. Abundant epidural scar formation has also been associated with the herniated disk itself, since peridiskal scar is seen even in previously unoperated patients [17]. This scar enhances with Gd-DTPA in a fashion similar to scar in postoperative spine patients. Absorption of protruded disk material has long been known to be associated with “loose granulation tissue,” which invades the herniated material with fibroblasts and many capillaries [18]. Neovascularity of the edge of disk material has been suggested as the only reliable histologic clue that disk prolapse has occurred [19]. One other factor of potential importance is the causal role of venous stasis in the production of epidural and intraneural fibrosis [20]. Peri- and intraneural fibrosis have been linked to compression and distortion of the epidural plexus by disk herniations and hypertrophic bone changes, with direct compressive effects upon the nerves being much less frequent. All these changes (edge neovascularity, granulation tissue, peri- and intraneural fibrosis) would be ex-

pected to enhance with Gd-DTPA and to occur in anterior epidural structures.

In contrast to the tumultuous milieu of the anterior epidural space, posterior epidural scar is at a relatively remote site from the influence of the intervertebral disk. This might provide a pristine environment to allow development of the full maturation potential of scar (i.e., abundant collagen with little vascularity), which would demonstrate minimal contrast enhancement. Further evidence of the stability of the posterior epidural region in this dog model is seen in the two cases in which metaplastic cartilage was present intermixed with scar.

This study suggests that an appropriate model for epidural scar that has similar imaging characteristics to human epidural scar necessitates an extensive lumbar laminectomy with anterior epidural dissection. A simple laminectomy alone, while easily performed and commonly used, does not provide a physiologically correct time course of enhancement.

REFERENCES

- Langenskiöld A, Kiviluoto O. Prevention of epidural scar formation after operations on the lumbar spine by means of free fat transplant. *Clin Orthop* 1976;115:92-95
- Ketchum LD. Effects of triamcinolone on tendon healing and function: a laboratory study. *Plast Reconstr Surg* 1971;47:472-482
- Ketchum LD, Robinson DW, Waters FW. Follow up on treatment of hypertrophic scars and keloids with triamcinolone. *Plast Reconstr Surg* 1971;48:256-259
- Rydell N. Decreased granulation tissue reaction after installation of hyaluronic acid. *Acta Orthop Scand* 1970;41:307-311
- LaRocca H, Macnab I. The laminectomy membrane: studies in its evolution, characteristics, effects and prophylaxis in dogs. *J Bone Joint Surg* 1974;56B:545-550
- Jacobs RR, McClain O, Neff J. Control of post laminectomy scar formation: an experimental and clinical study. *Spine* 1980;5(3):223-229
- Teplick JG, Haskin ME. Computed tomography of the post-operative lumbar spine. *AJR* 1983;141:865-884
- Burton CV, Kirkaldy-Willis WH, Yong-Hing K, Heithoff KB. Causes of failure of surgery on the lumbar spine. *Clin Orthop* 1981;157:191-199

9. Meyer JD, Latchaw RE, Ropollo HM, Ghoshhajra K, Deeb ZL. Computed tomography and myelography of the postoperative lumbar spine. *AJNR* **1982**;3:223-228
10. Schubiger O, Valavanis A. Postoperative lumbar CT: technique results and indications. *AJNR* **1983**;4:595-597
11. Teplick JG, Haskin ME. Intravenous contrast-enhanced CT of the postoperative lumbar spine. Improved identification of recurrent disk herniation, scar, arachnoiditis, and diskitis. *AJNR* **1984**;5:373-383, *AJR* **1984**;143:845-855
12. Bundschuh CV, Modic MT, Ross JS, Masaryk TJ, Bohlman H. Epidural fibrosis and recurrent disk herniation in the lumbar spine: assessment with magnetic resonance. *AJNR* **1988**;9:169-178
13. Hochhauser L, Kieffer SA, Cacayorin ED, Petro GR, Teller WF. Recurrent postdiscectomy low back pain: MR-surgical correlation. *AJNR* **1988**;9:769-774
14. Hueftle MG, Modic MT, Ross JS, et al. Lumbar spine: postoperative MR imaging with Gd-DTPA. *Radiology* **1988**;167:817-824
15. Ross JS, Delamarter R, Aikawa M, et al. Gadolinium-DTPA-enhanced MR imaging of the postoperative lumbar spine: time course and mechanism of enhancement. *AJNR* **1989**;10:37-46, *AJR* **1989**;152:825-834
16. McGraw WT, Ten Cate AR. Role for collagen phagocytosis by fibroblasts in scar remodeling. An ultrastructural stereologic study. *J Invest Dermatol* **1983**;81:375-378
17. Montanez J, Masaryk TJ, Ross JS, et al. Gd-DTPA: use in the unoperated spine. Presented at the annual meeting of the American Society of Neuroradiology, Chicago, May **1988**
18. Lindblom K, Hultqvist G. Absorption of protruded disk tissue. *J Bone Joint Surg* **1950**;32A(3):557-560
19. Weidner N, Rice DT. Intervertebral disk material: criteria for determining probable prolapse. *Hum Pathol* **1988**;19(4):406-410
20. Hoyland J, Freemont AJ, Jayson MI. New pathogenic mechanism for periradicular fibrosis (abstr). Presented at the annual meeting of the Pathologic Society of Great Britain and Ireland, University of Newcastle upon Tyne, July **1988**